

# EROSION WEAR RESISTANCE OF TITANIUM-MATRIX COMPOSITE Ti/TiN PRODUCED BY DIODE-LASER GAS NITRIDING

## ODPORNOST KOMPOZITA PROTI EROZIJSKI OBRABI Ti/TiN IZDELANEGA S PLINSKIM NITRIRANJEM S POMOČJO DIODNEGA LASERJA

Aleksander Lisiecki<sup>1</sup>, Agnieszka Kurc-Lisiecka<sup>2</sup>

<sup>1</sup>Silesian University of Technology, Faculty of Mechanical Engineering, Welding Department, Konarskiego 18A, 44-100 Gliwice, Poland

<sup>2</sup>University of Dąbrowa Górnicza, Rail Transport Department, Ciepłaka 1c, 41-300 Dąbrowa Górnicza, Poland  
aleksander.lisiecki@polsl.pl

*Prejem rokopisa – received: 2015-06-30; sprejem za objavo – accepted for publication: 2016-02-05*

doi:10.17222/mit.2015.160

A prototype experimental stand equipped with a novel high-power direct diode laser (HPDDL), characterized by unique properties of the laser beam, was applied for producing titanium-matrix composite (TMC) surface layers during the laser gas nitriding (LGN) of the titanium alloy Ti6Al4V in the liquid state. The erosion wear characteristic of the substrate and nitrided surface layers was investigated. It was found that the erosion wear resistance of the composite surface layers is significantly higher than the substrate of titanium alloy Ti6Al4V. The erosion wear resistance depends on the angle of incidence. Reducing the angle of incidence decreases the weight loss of the composite surface layers and simultaneously increases the weight loss of the Ti6Al4V. It was found that the weight loss of the composite surface layer with the highest resistance is over six times lower compared to the Ti6Al4V, at an incident angle of 15°.

Keywords: laser nitriding, titanium alloy, diode laser, erosion wear, composite

Prototipno eksperimentalno stojalo opremljeno z novim diodnim laserjem velike moči (HPDDL), značilnem po edinstvenih lastnostih laserskega žarka, je bilo uporabljeno za izdelavo površinske plasti kompozita na osnovi titana (TMC), med plinskim nitriranjem z laserjem (LGN) titanove zlitine Ti6Al4V, v staljenem stanju. Preiskovane so bile značilnosti erozijske obrabe podlage in nitrirane površine. Ugotovljeno je bilo, da je odpornost na erozijsko obrabo kompozitne površinske plasti občutno večja v primerjavi s podlago iz titanove zlitine Ti6Al4V. Odpornost na erozijsko obrabo je odvisna od vpadnega kota. Zmanjšanje vpadnega kota zmanjšuje izgubo teže površinske kompozitne plasti in hkrati poveča izgubo teže Ti6Al4V. Ugotovljeno je, da je izguba teže kompozitne površinske plasti, z največjo odpornostjo, pri vpadnem kotu 15°, več kot šestkrat manjša v primerjavi z Ti6Al4V.

Ključne besede: nitriranje z laserjem, titanova zlitina, diodni laser, erozijska obraba, kompozit

## 1 INTRODUCTION

Titanium alloys, thanks to their excellent strength-to-weight ratio and excellent corrosion resistance, are widely used in aerospace, automotive, power plant, maritime, and many other industries.<sup>1-6</sup> The most commonly used titanium alloy is Ti6Al4V (Grade 5 according to ASTM). Light metals and alloys are of particular importance in aerospace. For example, more than half of the rotating parts of a modern turbofan aircraft engine are made of titanium alloys, including the rotors and fan blades.<sup>7-9</sup> Similarly, the blades made of titanium alloys are commonly used in the steam turbines of high-power generators.<sup>10-13</sup> Titanium alloys are also used for manufacturing parts for turbochargers, air and hydraulic pumps, turbines and impellers, etc.<sup>14-16</sup> In each of the above cases, the working surfaces are exposed to wear, mainly by erosion or cavitation erosion.<sup>1,17</sup> For example, the engines of planes, helicopters, and other aircraft, as well as rocket engines are often subjected to severe erosion from sand and dust particles, drops of

rain, or other solid and hard particles in flight and also during manoeuvres at the airport or landing pad.<sup>18-20</sup>

However, titanium alloys, and particularly pure titanium, do not possess high resistance to erosive wear because of the relatively low surface hardness.<sup>1-6</sup> Therefore, various methods to modify the surface of the titanium alloys are used in industry, and also new methods and techniques are being developed.<sup>1-6,21</sup>

Among the many methods of surface modification of titanium alloys, one of the most efficient is laser gas nitriding (LGN).<sup>2</sup> Y. Fu et al.<sup>2</sup> have studied different methods for improving the erosion resistance of pure titanium. They have found that the laser surface treatment of titanium in a nitrogen atmosphere provides the best results and a significant improvement of the erosion resistance compared to other methods of surface treatment and the deposition of surface layers.<sup>2</sup>

Although the LGN method was invented in 1983, it is still being developed. The reason for this is the continuous development of laser devices and associated with this advances in laser technology.<sup>1,4</sup> The LGN process for

titanium and titanium alloys has been widely studied by scientists, and also there are plenty of articles in this field. However, most of the articles concern the structure, morphology, corrosion resistance, tribology and mechanical properties of the surfaced layers produced by gaseous CO<sub>2</sub> and solid-state YAG lasers.<sup>4,22</sup> There are only a few publications on the application of high-power diode lasers (HPDLs) in the process of titanium nitriding and also there is no information on the erosion wear resistance of surface layers nitrided by HPDLs.<sup>23–25</sup>

In the present work, a novel continuous wave (CW) HPDL emitted in the near-infra-red band at 808 nm, with a rectangular laser beam spot and a uniform energy distribution across the spot was applied for producing surface layers on the titanium alloy Ti6Al4V during LGN. The erosion wear resistance of the Ti6Al4V alloy before and after the LGN process at different angles of incidence was investigated.

## 2 EXPERIMENTAL PART

The titanium alloy Ti6Al4V (Grade 5 according to ASTM B265) with the nominal chemical composition 6.29 Al, 4.12 V, 0.14 C, 0.18 Fe in % of mass fractions and balance Ti was chosen for investigations of the nitriding process. The specimens of titanium alloy for the nitriding tests and for the erosion tests were cut into coupons 50.0×100.0 mm from a hot-rolled sheet having a thickness of 3.0 mm. The specimens of titanium alloy used for the erosion tests were mechanically ground by 180-grit SiC paper and cleaned. In turn, the specimens for LGN tests were mechanically ground and degreased with acetone prior to the nitriding tests.

The trials of LGN were carried out by means of a fully automated prototype stand equipped with a novel high-power direct diode laser (HPDDL) characterized by direct emission of the laser beam, rectangular laser-beam spot with a width of 1.8 mm and a length of 6.8 mm at a given configuration of optics and a short wavelength of 808 nm.

The short wavelength is advantageous because of the efficiency of the heat transfer to the metal surface as a result of Fresnel absorption. In this case the absorption coefficient on the surface of the titanium alloy for the 808 nm wavelength is significantly higher compared to the wavelength of gaseous CO<sub>2</sub> lasers and even compared to the solid-state lasers. Additionally, the multi-mode and even energy distribution of the laser radiation along the longer side of the beam spot ensures the uniform irradiation of the laser-treated surface and a uniform temperature distribution across the processing track.<sup>4</sup> In order to ensure the full control of the processing atmosphere, the samples were placed in a nitrogen-filled chamber. The pure nitrogen (99.999 % purity) was supplied into the chamber at flow rate of 10.0 L/min and a pressure of 1.0 atm. The nitrogen flow was switched in advance of about 90 s to remove the air from the

chamber. The laser beam was delivered into the chamber through a transparent cover made of tempered glass. The rectangular beam was focused on the top surface of the specimens and the beam spot was set transversely to the scanning direction. The test surface layers were produced as single stringer beads during linear scanning of the surface by the laser beam in a pure nitrogen atmosphere. The test surface layers were produced at different processing parameters, and thus a different heat input of nitriding. The processing parameters are given in **Table 1**.

**Table 1:** Parameters of the laser gas nitriding of the titanium alloy Ti6Al4V by the HPDDL

**Tabela 1:** Parametri plinskega nitriranja z laserjem titanove zlitine Ti6Al4V z HPDDL

No. of surface layer	Scanning speed, mm/min	Laser output power, W	Heat input, J/mm	Power density, kW/cm <sup>2</sup>
S1	200	1000	300	8.17
S2	200	800	240	6.54
S3	200	600	180	4.90

The erosion tests were performed in accordance with the ASTM G76 standard for a determination of the erosion rate by solid particles' impingement in a gas stream. The apparatus used to carry out the erosion tests was built strictly in accordance with the requirements of the standard. The solid particles used for the erosion tests were natural angular alumina sands with a size of 50 μm. The erodent particles were fed from a disk powder feeder and accelerated from a nozzle by pressured dry air. The pressured air was supplied from a cylinder and the pressure was stabilized by a two-stage pressure reducer. The air pressure was adjusted to provide the particle velocity of 70 m/s. The feed rate of the abrasive sand was set at 2.0 g/min. The distance from the nozzle tip to the tested surface was kept at 10.0±0.5 mm. A nozzle having an inner diameter of 1.5 mm and a length of 50 mm was applied. A rotary sample holder allowed for a change in the angle of the particles' impingement on the surface from 15° to 90°. Prior to the erosion test of the surface layers and the base metal, a calibration of the particles' velocity was performed according to the procedure given in the ASTM G76 standard. The material used for the calibration was C22 annealed steel, according to EN 10250-2 (1020 steel according to AISI).

All the erosion tests were performed under ambient conditions with a temperature of about 25 °C and a relative humidity of 45–50 %.

The base metal Ti6Al4V titanium alloy and the surface layers were eroded for 5 and 10 minutes at impact angles of 15°, 30°, 45° and 90°.

The weight of the samples was measured before and after the erosion test using a laboratory scale with an accuracy of ±0.01 mg. Prior to the measurements of weight, each sample was cleaned with compressed air and the weight was measured three times in order to

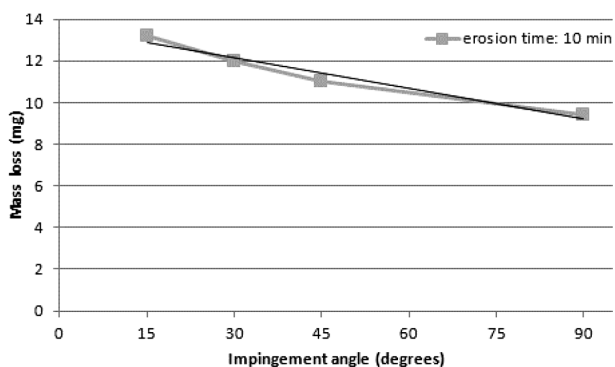


**Figure 1:** Relationship between the mass loss and impingement angle for erosion of the base metal Ti6Al4V

**Slika 1:** Odvisnosti med izgubo mase in vpadnim kotom pri eroziji osnovne kovine Ti6Al4V

determine the mean value and to provide the high accuracy of the measurement.

Subsequently, the eroded surfaces were analysed with a scanning electron microscope (SEM) to identify the mechanisms of wear and mass loss.

### 3 RESULTS AND DISCUSSION

The relationship between the mass loss and the impingement angle after 10 min of erosion test of the base metal Ti6Al4V is shown in **Figure 1**. As can be seen, the mass loss of the base metal is clearly dependent on the angle of alumina particles' impact (impingement angle), and the mass loss increases with a decreasing the angle. Such dependence is typical for ductile materials, as indicated in the literature.<sup>1-3</sup>

On the other hand, in the case of the laser gas nitrided surface layers the relationship between the mass loss and impingement angle is different, as can be seen in **Figure 2**. For all of the nitrided surface layers the lowest mass loss occurred at the lowest impingement angle of 15°, while increasing of the angle resulted in increasing of the mass loss, reaching the maximum at an angle of 90°, as shown in **Figure 2**. Thus in general, the nitrided surface layers exhibited brittle-type behaviour, characteristic for hard and brittle materials.<sup>1-3</sup> The obtained results are different from those presented by J. R. Laguna-Camacho et al.<sup>3</sup> in the case of TiN coatings deposited by PVD on the substrate of steel. In addition, the data in **Figure 2** indicate a clear relationship between the laser processing parameters and the erosion behaviour of the nitrided surface layers. For example, the surface layer produced at the lowest laser output power of 600 W (Sample S3) and so the lowest heat input of 180 J/mm exhibited the lowest mass loss so the best erosion resistance ( $R_e$ ) at the highest angle of 90°, as can be seen in **Figure 2a**. In this case the mass loss was about 5 mg. In contrast, the surface layer produced at the highest heat input of 300 J/mm (laser power 1000 W, Sample S1) exhibited the highest mass loss of about 8 mg, (**Figure 2c**). For comparison, the surface layer produced at the medium heat

input of 240 J/mm (Sample S2) also showed a medium mass loss below 7 mg, (**Figure 2b**). Here, it is possible to conclude that in the range of the investigated parameters the erosion resistance of the laser nitrided surface layers at the impingement angle of 90° is almost directly proportional to the heat input of the LGN process. This phenomenon can be explained by the differences in the microstructure of the surface layers nitrided at different parameters (heat inputs). At a high impingement angle (e.g., 90°) the particles impact both the hard TiN nitrides and the softer metallic matrix. So in this case the mass loss, thus the erosion resistance  $R_e$ , is dependent on the properties of the titanium nitrides' precipitations (brittle material type), but equally on the properties of the metallic matrix (a rather ductile material type). SEM micro-

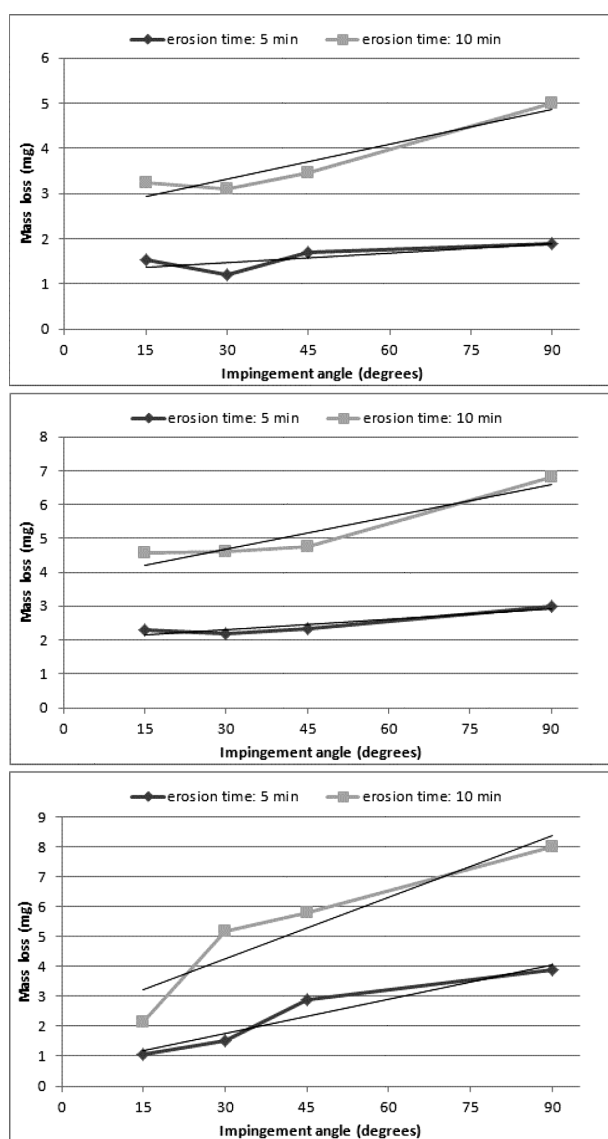


**Figure 2:** Relationship between the mass loss and impingement angle for different erosion times of the nitrided surface layers: a) S3, b) S2 and c) S1

**Slika 2:** Odvisnost med izgubo mase in vpadnim kotom pri različnih časih erozije nitrirane površinske plasti: a) S3, b) S2 in c) S1

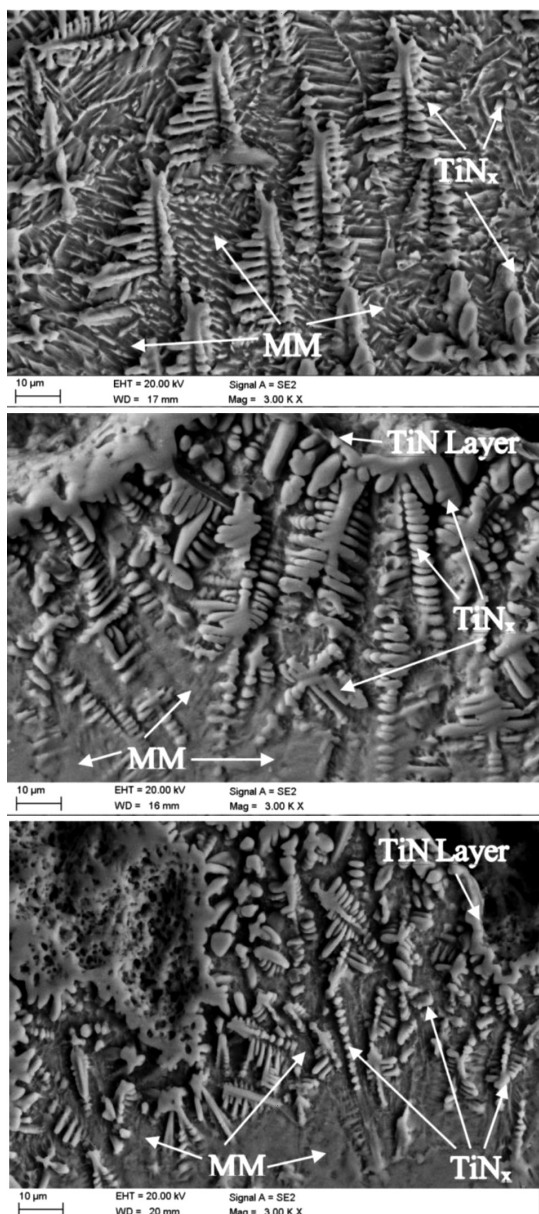


**Figure 3:** SEM micrographs of the nitrated surface layers, showing the composite structure consisting of  $TiN_x$  dendrites in a metallic matrix of samples: a) S1, b) S2 and c) S3; TiN Layer – a homogenous layer of titanium nitrides on the top surface, MM – metal matrix of  $Ti\alpha(N)$ ,  $TiN_x$  – titanium nitrides precipitation with various stoichiometric concentration ( $\delta-TiN$ ,  $\epsilon-Ti_2N$ )

**Slika 3:** SEM-posnetek nitrirane površinske plasti, ki kaže kompozitno strukturo, ki sestoji iz  $TiN_x$  dendritov v kovinski osnovi vzorcev: a) S1, b) S2 in c) S3; TiN plast – homogena plast titanovih nitridov na površini, MM – kovinska osnova  $Ti\alpha(N)$ ,  $TiN_x$  – izločanje titanovih nitridov z različno stehiometrično koncentracijo ( $\delta-TiN$ ,  $\epsilon-Ti_2N$ )

graphs of the nitrated surface layers at the same magnification are presented in **Figure 3**. As can be seen, the morphology and size of the TiN dendrites, as well as the proportion between the nitrides (population) and the metallic matrix, are different for every surface layer. The microstructure and morphology of every single surface layer correlate with the microhardness profile on the

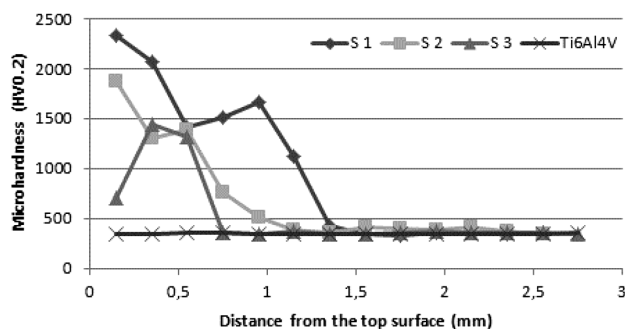


**Figure 4:** Microhardness distribution on the cross-section of nitrated surface layers and the base metal of titanium alloy Ti6Al4V

**Slika 4:** Razporeditev mikrotvrdote na preseku nitrirane površinske plasti in osnovne kovine, titanove zlitine Ti6Al4V

cross-section, (**Figure 4**). The surface layer produced at the highest heat input of 300 J/mm is composed of long and densely packed TiN dendrite precipitations with a relatively small amount of metallic matrix (**Figure 3a**). Therefore, the microhardness in this case reaches the maximum value and remains at a high level to a depth of about 1.4 mm, (**Figure 4**). The high amount of TiN dendrites characterized by a very high microhardness is responsible for the erosion behaviour of the surface layer at the angle of  $90^\circ$ . In turn, the nitrated surface layers produced at lower heat inputs have fewer TiN dendrite precipitations (**Figure 3b, c**). Additionally, these surface layers are thinner and also the size of the TiN dendrites is smaller and the share of metallic matrix is significantly higher. These differences in the structure and morphology of the surface layers cause a change in the microhardness distribution as well as in the erosion behaviour (**Figure 2, 4**). In this case, the softer metallic matrix has a greater influence on the erosion wear mechanism (erosion behaviour).

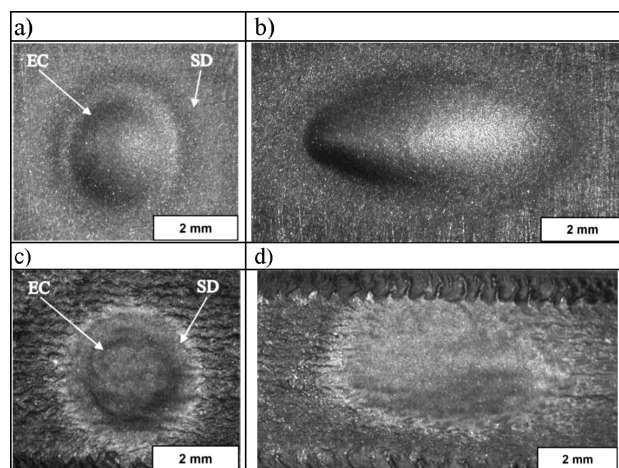


**Figure 5:** A view of eroded surfaces of titanium alloy Ti6Al4V at the incident angle of: a)  $90^\circ$  and b)  $15^\circ$  and nitrated surface layer S1 eroded at the incident angle of c)  $90^\circ$  and d)  $15^\circ$ ; EC – erosion crater, SD – secondary damage ("halo effect")

**Slika 5:** Izgled erodirane površine titanove zlitine Ti6Al4V pri vpadnem kotu: a)  $90^\circ$  in b)  $15^\circ$  in nitrirana površinska plast S1, erodirana pri vpadnem kotu c)  $90^\circ$  in d)  $15^\circ$ ; EC – erozijski krater, SD – sekundarne poškodbe ("halo efekt")

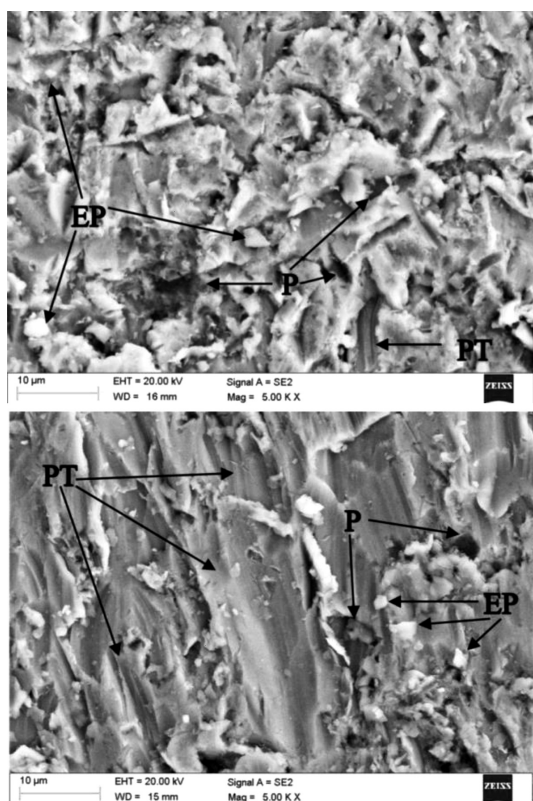


**Figure 6:** SEM morphology of the bottom surface of eroded craters of titanium alloy Ti6Al4V at the incident angle of: a) 45° and b) 15°; P – pits, PT – ploughing trenches, EP – erodent particles

**Slika 6:** SEM morfologija površine dna kraterja titanove zlitine Ti6Al4V, pri vpadnem kotu, a) 45° in b) 15°; P – jamice, PT – brazde, EP – delci nastali pri eroziji

On the other hand, in the case of the lowest impingement angle of 15°, the surface layer produced at the maximum heat input, having the maximum depth and maximum microhardness, exhibited the lowest mass loss, and thus the highest erosion resistance  $R_e$ , (Figure 2c). However, the relationship between the mass loss at the angle of 15° and the processing parameters of the LGN process (in general, the heat input) is not as clear and simple as in the case of the angle 90°. The reason for this is the different way of impacting the surface by the alumina erodent particles. When the erosive stream impacts the surface at a low angle of 15°, the alumina particles are partially bounced and slide on the top surface. In such conditions the erosive wear of the composite surface layer is limited by the erosion rate of the hard and wear-resistant titanium nitride precipitations, and the softer metal matrix is not exposed to such strong erosion as at high angles of impact. Thus, the amount of metallic matrix has less effect on the overall erosion rate at a low angle of impact. The eroded craters produced at different incident angles on the surface of the titanium alloy Ti6Al4V and on the nitrided surface layers are shown in Figure 5. The shape and area of the craters depend on the incident angle. The circular craters characterized by the smallest area were produced at an angle of 90°. The increase in the erosion angle changes the shape of the

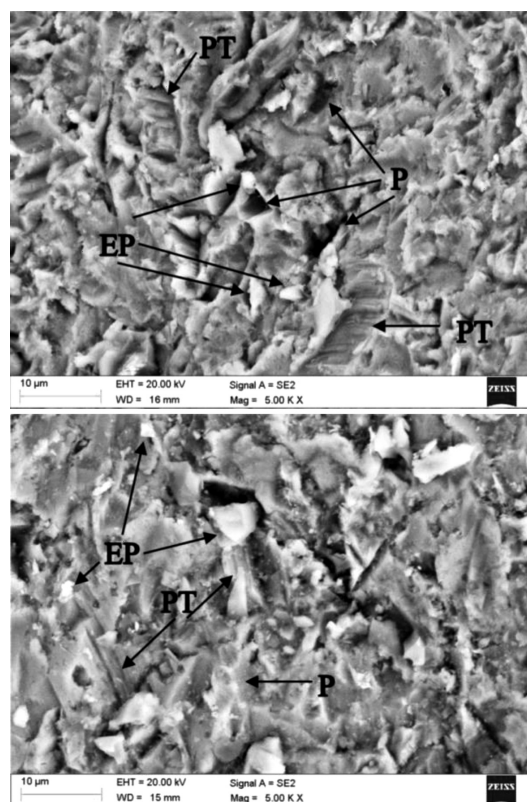


**Figure 7:** SEM morphology of the bottom surface of eroded craters of nitrided surface layer S1 at the incident angle of 90° a) and 15° b); P – pits, PT – ploughing trenches, EP – erodent particles

**Figure 7:** SEM morfologija površine dna erozijskega kraterja na nitrirani površinski plasti S1, pri vpadnem kotu a) 90° in b) 15°; P – jamice, PT – brazde, EP – delci nastali pri eroziji

crater to an elliptical shape and simultaneously increases the wear area. The secondary erosion damage zone can be observed around the deep eroded craters (Figure 5). This secondary damage is caused by the scattered particles of the erodent stream. This phenomenon is called, in the literature, the "halo effect".<sup>3</sup>

The SEM morphology of the bottom surface of the eroded craters is shown in Figure 6, 7. The worn surfaces of the titanium alloy Ti6Al4V eroded at high incident angles show irregular indentations, craters and deep pits (Figure 6a). Additionally, fragments of erodent particles embedded in the surface were identified in the bottom of the eroded craters (Figure 6a). On the other hand, the worn surfaces eroded at low incident angles show deep and long scratches and plastically deformed ploughing trenches (Figure 6b). Besides the fragments of erodent particles embedded in the surface, also some wear debris inside the trenches were found. The appearance of the eroded surfaces and traces of wear indicate two different mechanisms of wear during erosion at low and high incident angles. At low incident angles the material loss is mainly caused by the abrasive wear by plastic deformation of the material, cutting and ploughing the surface by the angular erodent particles. In turn, at high incident angles, the material loss is mainly caused by plastic deformation and extrusion of the ma-

terial. The worn surface morphology of the nitrided surface layer eroded at a low incident angle is clearly different compared to the base metal of titanium alloy, as can be seen in **Figure 7b**. In this case the ploughing trenches are shorter because the erodent particles rebound from the hard surface. Large erodent particles embedded in the surface were also found. The worn surface of the nitrided surface layer eroded at a high angle were more roughened with pits and craters, but without traces of cracks (**Figure 7a**). The erodent particles embedded in the surface were found also. In this case the material loss is caused by brittle ruptures of the composite layer, especially the hard TiN precipitations.

#### 4 CONCLUSIONS

The base metal of titanium alloy Ti6Al4V exhibited ductile-type behaviour, reaching the maximum erosion rate at the lowest angle of 15° of the alumina particles' impact. Unlike the titanium alloy, the nitrided surface layers exhibited brittle-type behaviour, reaching the maximum erosion rate at the high angle of 90°. Nevertheless, the erosion resistance ( $R_c$ ) of the nitrided surface layers is higher for all the angles of impingement compared to the base metal of titanium alloy. Additionally, in the range of the investigated processing parameters, the heat input of the LGN process has a strong influence on the microstructure, morphology and microhardness distribution across the surface layers, and also on the erosion behaviour, especially at the angle of 90°. It was found that the erosion rate of the composite surface layers at an angle of 90° depends on the properties of hard nitrides and the softer metal matrix equally. In turn, the erosion rate of the composite surface layers at a low angle of 15° depends mainly on the properties of the hard nitride precipitations. In this case the amount and properties of the metallic matrix has less effect on the overall erosion rate.

#### 5 REFERENCES

- H. C. Man, Z. D. Cui, T. M. Yue, F. T. Cheng, Cavitation erosion behavior of laser gas nitrided Ti and Ti6Al4V, *Mat. Sci. Eng. A*, 355 (2003), 167–173, doi:10.1016/S0921-5093(03)00062-5
- Y. Fu, H. Du, Y. Gu, Improvement of Erosion Resistance of Titanium with Different Surface Treatments, *J. Mater. Eng. Perf.*, 9 (2000), 571–579
- J. R. Laguna-Camacho, J. E. Escalante-Martínez, R. Cruz-Vicencio, J. V. Méndez-Méndez, I. Arzate-Vázquez, I. Hernández-Romero, M. Vite-Torres, Solid Particle Erosion Behaviour of TiN Coating on AISI 4140 Steel, *J. Surf. Eng. Mat. Adv. Tech.*, 4 (2014), 1–8, doi:10.4236/jsemat.2014.41001
- A. Lisiecki, Titanium Matrix Composite Ti/TiN Produced by Diode Laser Gas Nitriding, *Metals*, 5 (2015), 54–69, doi:10.3390/met5010054
- I. Mitelea, E. Dimian, I. Bordeasă, C. Crăciunescu, Cavitation Erosion of Laser-Nitrided Ti–6Al–4V Alloys with the Energy Controlled by the Pulse Duration, *Tribol. Lett.*, 59:31 (2015), 1–9, doi:10.1007/s11249-015-0558-6
- M. Dhanda, B. Haldar, P. Saha, Development and Characterization of Hard and Wear Resistant MMC Coating on Ti-6Al-4V Substrate by Laser Cladding, *Proceed. Mater. Sci.*, 6 (2014), 1226–1232
- A. Lisiecki, Welding of titanium alloy by Disk laser, *Proc. of SPIE Vol. 8703, Laser Technology 2012: Applications of Lasers*, 87030T (January 22, 2013), doi:10.1117/12.2013431
- A. Lisiecki, Welding of thermomechanically rolled fine-grain steel by different types of lasers, *Arch. Metall. Mater.*, 59 (2014), 1625–1631, doi:10.2478/amm-2014-0276
- A. Kurc-Lisiecka, Wojciech Ozgowicz, Wiktoria Ratuszek, Joanna Kowalska, Analysis of deformation texture in AISI 304 steel sheets, *Sol. St. Phenom.*, 203–204 (2013), 105–110, doi:10.4028/www.scientific.net/SSP.203-204.105
- R. Burdzik, L. Konieczny, Z. Stanik, P. Folega, A. Smalcerz, A. Lisiecki, Analysis of impact of chosen parameters on the wear of camshaft, *Arch. Metall. Mater.*, 59 (2014), 957–963, doi:10.2478/amm-2014-0161
- J. Kusiński, S. Kac, A. Kopia, A. Radziszewska, M. Rozmus-Górnkowska, B. Major, L. Major, J. Marczak, A. Lisiecki, Laser modification of the materials surface layer – a review paper, *Bull. Pol. Acad. Sci. Tech. Sci.*, 60 (2012), 711–728, doi:10.2478/v10175-012-0083-9
- J. Górka, Weldability of thermomechanically treated steels having a high yield point, *Arch. Metall. Mater.*, 60 (2015), 469–475
- R. Burdzik, T. Węgrzyn, Ł. Konieczny, A. Lisiecki, Research on influence of fatigue metal damage of the inner race of bearing on vibration in different frequencies, *Arch. Metall. Mater.*, 59 (2014), 1275–1281, doi:10.2478/amm-2014-0218
- A. Grajcar, M. Rożański, S. Stano, A. Kowalski, Microstructure characterization of laser-welded Nb-microalloyed silicaluminum TRIP steel, *J. Mater. Eng. Perform.*, 23 (2014), 3400–3406
- J. Górka, Changes in the structure and properties of the steel S700MC by heat treatment, *Adv. Mat. Res.*, 1036 (2014), 111–116
- T. Węgrzyn, J. Piwnik, D. Hadryś, R. Wieszała, Car body welding with micro-jet cooling, *J. Arch. Mater. Sci. Eng.*, 49 (2011), 90–94
- A. Grajcar, M. Rożański, S. Stano, A. Kowalski, B. Grzegorzczak, Effect of Heat Input on Microstructure and Hardness Distribution of Laser Welded Si-Al TRIP-Type Steel, *Adv. Mater. Sci. Eng.*, 2014 (2014), doi.org/10.1155/2014/658947
- B. Oleksiak, G. Siwiec, A. Blacha-Grzechnik, J. Wieczorek, The obtained of concentrates containing precious metals for pyrometallurgical processing, *Metalurgija* 53 (2014), 605–608
- D. Janicki, High power diode laser cladding of wear resistant metal matrix composite coatings, *Sol. St. Phenom.*, 99 (2013), 587–592
- J. Słania, Influence of phase transformations in the temperature ranges of 1250-1000 °C and 650-350 °C on the ferrite content in austenitic welds made with T 23 12 LRM3 tubular electrode, *Arch. Metall. Mater.*, 50 (2005), 757–767
- Z. Brytan, M. Bonek, L. A. Dobrzański, W. Pakielna, Surface Layer Properties of Sintered Ferritic Stainless Steel Remelted and Alloyed with FeNi and Ni by HPDL Laser, *Adv. Mat. Res.*, 291-294 (2011), 1425–1428, doi:10.4028/www.scientific.net/AMR.291-294.1425
- M. Muszyfaga-Staszuk, L.A. Dobrzański, S. Rusz, M. Staszuk, Application examples for the different measurement modes of electrical properties of the solar cells *Arch. Metall. Mater.*, 59 (2014), 247–252
- D. Janicki, Disk Laser Welding of Armor Steel, *Arch. Metall. Mater.*, 59 (2014), 1641–1646, doi:10.2478/amm-2014-0279
- B. Słazak, J. Słania, T. Węgrzyn, A. P. Silva, Process Stability Evaluation of Manual Metal Arc Welding Using Digital Signals, *Mater. Sci. Forum*, 730-732 (2013), 847–852
- M. Staszuk, L. A. Dobrzański, T. Tański, W. Kwaśny, M. Muszyfaga-Staszuk, The effect of PVD and CVD coating structures on the durability of sintered cutting edges, *Arch. Metall. Mater.*, 59 (2014), 269–274